Saturation and pressure inference from velocities and density

Fernando Moraes, Universidade Estadual do Norte Fluminense, Brazil
Colin MacBeth, Heriot Watt University, United Kingdom

This paper was prepared for presentation at the 9th International Congress of the Brazilian Geophysical Society held in Salvador, Brazil, 11-14 September 2005.

Abstract

We present a Bayesian formulation for the inference of saturation and pressure from seismic attributes, using Gassmann's equations in connection with a dry frame pressure sensitivity law. Laboratory data is analyzed for the most representative pressure sensitivity parameters. A 1D inversion example on synthetic data illustrates how the methodology works.

Introduction

Time lapse seismic is growing to become a standard tool for reservoir management because it provides an interpretation of hydrocarbon production effects, such as fluid movement, changes of pressure and temperature, and porosity reduction by compaction. Difficulties associated with the interaction of these multiple effects makes the majority of 4D case studies qualitative and non-unique in nature. However information produced from a 4D survey, such as images of the water-oil contact is used to history match against reservoir simulations. The latter is the ultimate quantitative method for reservoir management (MacBeth et al. 2005).

A considerable amount of effort has been placed in making time lapse seismic more quantitative. This is usually tackled on a case-by-case approach, where parameters affecting the seismic response are ranked according to their degree of significance. Eventually, the least influential parameters are dropped out from the solution. 4D anomalies are then modeled using only a few parameters. But if a parameter were to be singled out in terms of its general relevance, perhaps the choice would be saturation. It is of primary interest in virtually all cases because it provides a direct assessment of reservoir drainage pattern.

Pressure is highly coupled with saturation, acting either to reinforce or counteract saturation effects depending on the production strategy. Rising water saturation stiffens pore fluid, leading to an increase in bulk modulus as predicted by the Gassmann equation. Pore pressure increase leads to a decrease in differential pressure and consequently a decrease in both bulk and shear moduli (see e.g. MacBeth, 2004). Pore pressure increase also leads to stiffen the pore fluid itself. Natural production schemes are usually characterized by an increase in water saturation and pressure depletion. However, under forced drainage schemes increasing water saturation can be accompanied by pressure increase.

In normal consolidated sandstone reservoirs, porosity and rock frame density are expected to change by only a few percent (Khaksar et al., 1999). However, for specific cases such in chalk reservoirs, porosity becomes an important factor due to compactation. Other parameters, such as temperature are also highly relevant only in specific situations. For example, steam injection enhanced production schemes are mainly driven by temperature. The above perhaps explains why quantification of saturation and pressure effects has received wide attention in the recent research literature concerning the interpretation of time-lapse studies.

There are several published methodologies available for saturation and pressure determination (Tura and Lumley 1999, Landro 2001, Floricich and MacBeth 2005). This work aims at producing a contribution towards improving our understanding of the uncertainties involved in the inference of saturation and pressure from seismic attributes. It builds on previous work of porosity and clay volume inference presented by Loures and Moraes (2005) and porosity and saturation presented by da Costa et al. (2004), as discussed in the next section.

Method

Consider the problem of making inferences about oil saturation (S_o) and pressure (P) at a particular point, or homogeneous region in space, from multiple sets of data, represented by $\mathbf{d} = \{\mathbf{d}_1, \mathbf{d}_2, \mathrm{K}, \mathbf{d}_K \mid \mathbf{d}_i \in R^{N_i}, i = 1, \mathrm{K}, K\}$. To fully represent the parameter space, let $\mathbf{m} = (S_o, P)^T \in R^2$ and $\mathbf{h} = (h_1, \mathrm{K}, h_L)^T \in R^L$ be vectors representing saturation and pressure and the set of hyperparameters. Hyperparameters are additional parameters, which somehow need to be inferred from the data because they are necessary for implementing the calculations. These can come either from the data or statistical models involved in the formulation, as discussed below.

Following the Bayesian approach, the goal is to obtain the posterior distribution for saturation and pressure. A general form for the posterior distribution, covering the whole parameter space, can be written as

$$p(\mathbf{m}, \mathbf{h} \mid \mathbf{d}, I) = \frac{p(\mathbf{m}, \mathbf{h} \mid I)\, p(\mathbf{d} \mid \mathbf{m}, \mathbf{h}, I)}{p(\mathbf{d}, I)}, \qquad (1)$$

where $p(.)$ is generically used to denote a probability density function. The specific functional form is defined by context (i.e., the argument of the function). In the above equation (1), $p(\mathbf{m}, \mathbf{h} \mid I)$ is the joint *a priori* model for the saturation, pressure and the hyperparameters and $p(\mathbf{d} \mid \mathbf{m}, \mathbf{h}, I)$ is the likelihood function, carrying the forward modeling calculation. $p(\mathbf{d}, I)$ is the normalizing distribution required to maintain a total probability equal to unity. I

represents prior information, which is used to condition all probabilities. The final marginal posterior distribution for the desired parameters $\mathbf{m}$ can be computed by integration over the hyperparameters $\mathbf{h}$, which can be represented by

$$p(\mathbf{m}\,|\,\mathbf{d},I)=\frac{p(\mathbf{m}\,|\,I)}{p(\mathbf{d},I)}\int p(\mathbf{h}\,|\,I)\,p(\mathbf{d}\,|\,\mathbf{m},\mathbf{h},I)\,d\mathbf{h}, \qquad (2)$$

assuming the parameters $\mathbf{m}$ to be logically independent from hyperparameters $\mathbf{h}$.

As mentioned in the previous section, we are considering the information (data) from seismic velocities and density. Thus the data can be introduced either in its original form or by an appropriate transformation, such as bulk modulus (κ), shear modulus (μ) and density (ρ). After defining the data set containing relevant information about saturation and pressure, the standard steps of the Bayesian solution include: a) defining mathematical expressions relating data and parameters, and b) setting up the statistical models (prior and likelihood). Our approach closely follows da Costa et al. (2004), who present a Bayesian formulation for saturation inference based on Gassmann's equations. Here we also consider the effect of pressure as described by the formulae for the dry frame moduli derived by MacBeth (2004), which are given by

$$\kappa_d=\frac{\kappa_\infty}{1+E_\kappa e^{-P/P_\kappa}} \qquad (3)$$

$$\mu_d=\frac{\mu_\infty}{1+E_\mu e^{-P/P_\mu}}, \qquad (4)$$

each formula depending on the high-pressure asymptote (subscript ∞), a gradient parameter $E_{\kappa(\mu)}$ and a characteristic pressure $P_{\kappa(\mu)}$.

Other equations used are bulk density and Gassmann's, which increase the list of additional parameters to include:

- ϕ and Vsh, porosity and shale volume;
- κ_m and μ_m, the bulk and shear moduli of the solid (mineral) phase (sand-shale mixture);
- κ_w and κ_o, the fluid bulk moduli for water and oil phases;
- ρ_m, ρ_w and ρ_o, mineral, water and oil densities.

Next, we need to specify the probability models. We follow the same choices made by da Costa et al. (2004) to assume that errors are independent and Gaussian distributed with unknown uniform variances. This adds another additional 3 parameters to the set of hyperparameters, which are the data variances $\sigma_\kappa^2,\sigma_\mu^2$ and σ_ρ^2. The prior distribution is assumed to be approximately constant over the region where the likelihood shows significant amplitude.

Considering the above models, especially those relating data and parameters, the integral in equation (2) does not have a closed form solution. Alternative approaches to treat hyperparameters are to fix them as known quantities or to incorporate them as unknown variables in the inversion. Whereas the latter introduces additional non-uniqueness and complexity, most often requiring Monte Carlo type computational techniques, to fix them usually requires a prior stage of exploratory data analysis (data model set up and calibration). The calibration stage can be time consuming, but generally yields useful interpretations about the reservoir properties and its seismic response. The fixed hyperparameter approach can be equivalent to a more general solution to equation (2), if the calibration provides precise estimates of hyperparameters independently from other model parameters. For instance, if their distribution $p(\mathbf{h}\,|\,I)$ is sharply peaked, the marginal $p(\mathbf{m}\,|\,\mathbf{d},I)$ is equivalent to the conditional $p(\mathbf{m}\,|\,\mathbf{d},\mathbf{h}=\mathbf{h}_o,I)$. To check how our methodology works, we construct a synthetic 1D example based on laboratory and well log data from the Schiehallion reservoir, which is composed by Paleocene turbidite channels.

Laboratory data

Laboratory data consists of a set of measurements from 22 plugs collected from within reservoir sandstone zones. Measurements include mineralogy, porosity (He, effective and CMS), density (bulk, mineral and dry) and permeability, in addition to velocity (V_P and V_S) measurements as a function of confining pressure. Figure 1 shows the complete set of measurements expressed in terms of bulk and shear moduli. Laboratory elastic moduli is plotted against pressure and fitted by non-linear least squares to yield a range of pressure sensitivity curves, which are shown in Figure 1. Data points are plotted color coded by either porosity (ϕ, top row) or by shale volume (Vsh, bottom row). Colors show the correlation existing between porosity and pressure sensitivity, as reported by Dvorkin et al. (1996) and MacBeth (2004). Low porosity rocks appear more pressure sensitive than high porosity ones. However, Khaksar et al. (1999) present data showing the opposite trend.

Correlation of pressure sensitivity and shale volume, if at all present, is much less apparent (Figure 1). Khaksar et al. (1999) and MacBeth and Ribeiro (2005) presented detailed analysis on such correlations, by looking into individual pressure sensitivity parameters and support the idea of no significant link between total shale volume and pressure sensitivity. We select a representative pressure sensitivity curve by first analyzing porosity distribution over core samples. Figure 2 (a) show a bimodal probability density function for porosity. The data are separated according the porosity and the median is taken as the representative pressure sensitivity model. The selected models are plotted against conditional probability density functions computed over the (P,κ) and (P, μ) domains, given the various porosity values.

Inversion example

A 3 layer sand-shale model is constructed using similar sedimentary sequence and petrophysical parameters as given by the Schiehallion data set. Physical property profiles (Figure 3) are obtained, beginning with a pure sandstone model, whose effective elastic moduli and density are computed from a hypothetical matrix

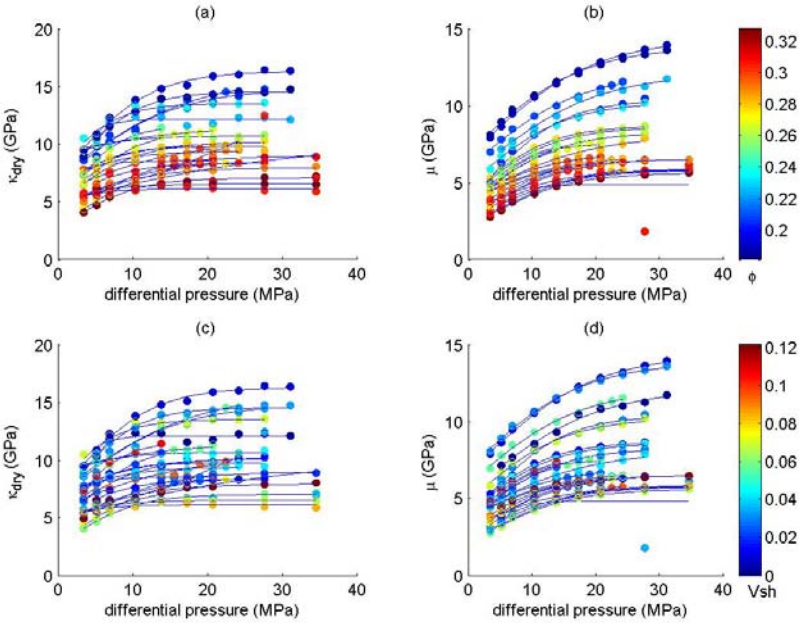

Figure 1 – Measured values of bulk and shear moduli as function of pressure taken from 22 room-dry sandstone plugs and best fitted models using equations (3) and (4). The plots at top row (a and b) are color coded with respect to effective porosity whereas (c) and (d) are color coded by shale volume. Note the high level of correlation between porosity and pressure sensitivity curves.

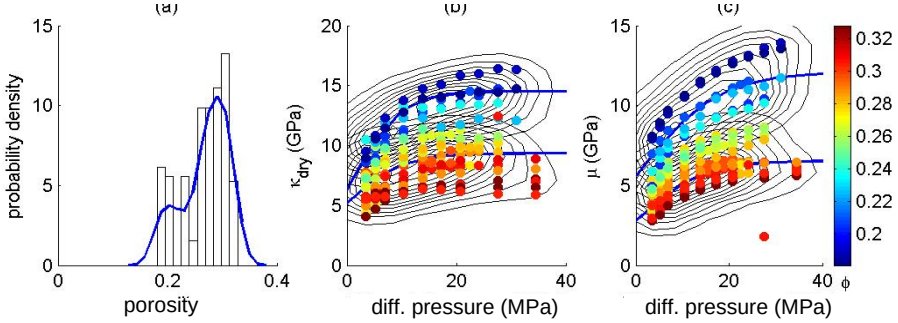

Figure 2 – Nonparametric probability density modeling for selected pressure sensitivity laws from core plug data.

L	facies	depth (m)	ϕ_{sand} (%)	Vsh (%)	saturation (%) (w,o,g)	P (MPa)
L1	A	0–32	15	5–100	100,0,0	20
	B	32–40	15	100	100,0,0	20
L2	A	40–55	30	3–1.5	20,80,0	15
	B	55–95	30	1.5	20,80,0	10
	C	95–110	30	1.5	100,0,0	10
L3	B,A	110–150	same as L1, but reversed with respect to depth			

Table 1 – Input parameters used to construct a 3 layer shale-sand model. Saturations and differential pressure profiles are given in the last two columns. The reservoir layer is L2. Figure 3 shows the actual distributions of porosity and shale volume.

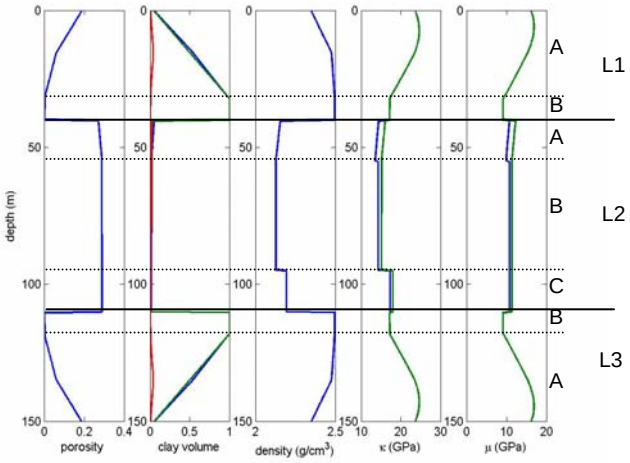

Figure 3 - Simulated porosity, clay volume, density and bulk and shear moduli profiles for the 3 layer model.

composition. The original sandstone is gradually replaced by a combination of shale and dispersed clays. The details of the model including variations in lithology, saturation and pressure are presented in Table 1 and Figure 3.

The synthetic data, consisting of V_P, V_S and density, are corrupted with Gaussian noise and inverted for saturation and pressure, using the Bayesian formulation presented in the previous section. Porosity and shale volume probability distributions are obtained according to the methodology described by Loures and Moraes (2005). Other parameters, such as mineral and fluid bulk and shear moduli and density are assumed known and as fixed values in inversion. Figure 4 shows the resulting marginal posterior distributions for saturation and pressure. The saturation and pressure of the central reservoir layer are well determined.

Pressure, which is set to values of 10MPa (top layer) and 15MPa (middle and bottom layers), seems to have lower associated uncertainty than saturation, as represented by the lower and upper limits of the 0.95 probability interval (Figure 4, b and d). Outside the reservoir, in the shaly sand layers, saturation tends to follow the shale trend whereas pressure remains close to the true trend at 20 MPa. The uncertainty grows large for both parameters as porosity decreases. Estimates (computed data) using saturation and pressure estimates fit the observed data very closely, even in the zero effective porosity intervals surrounding the reservoir (Figure 5) where the uncertainty is high.

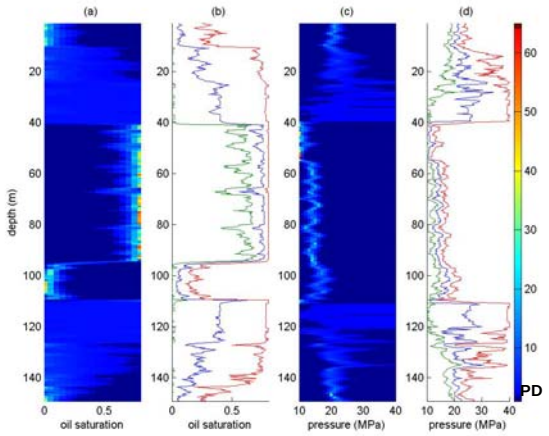

Figure 4 – Marginal posterior distributions (at each depth point) for oil saturation and pressure (a and c), and corresponding inference measure consisting of the mean (blue) and lower (green) and upper (red) limits for a 0.95 probability interval (b and d). Color scale represents probability density values (PD).

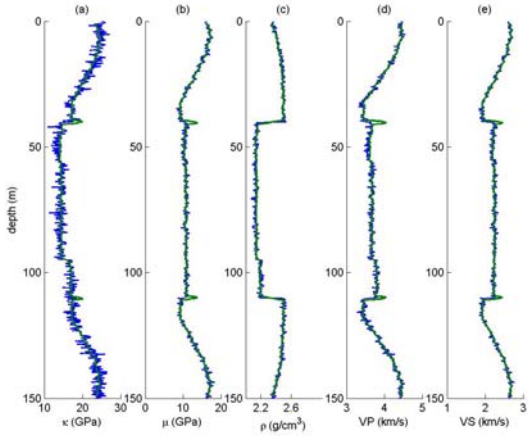

Figure 5 – Observed data (blue) and computed data (green) using mean saturation and pressure model estimates for elastic moduli (a and b), density (c) and velocities (d and e).

Conclusions

We presented a Bayesian formulation for saturation and pressure inference, which is able to incorporate data from multiple sources of information including laboratory and well log data. An extension for seismic attributes inverted from field data is possible. The large number of hyperparameters requires careful calibration or further extension to perform the numerical computations involved with equation (2).

Acknowledgment

This work received the financial support of Conselho Nacional de Desenvolvimento Científico e Tecnológico (CNPq) and the sponsors of Edinburgh Time Lapse Project, Heriot Watt University.

References

da Costa, E.F., Moraes, F.S. and Filho, N.P.F., 2004. Joint inference of porosity and saturation from multiple well logs. EAGE 66th Conference & Exhibition, Paris, France, Expanded abstract, 4 pp.

Dvorkin, J., Nur, A., Chaika, C., 1996, Stress sensitivity of Sandstones. Geophysics, **61**, 444-455.

Floricich, M., and MacBeth, C., 2005. Transforming 4D seismic to pressure and saturation using constraints from production data, *Second Annual Petroleum Conference and Exhibition, Cairo 2005.*

Khaksar, A., Griffiths, C.M., and McCann, C., 1999, Compressional and shear-wave velocities as a function of confining stress in dry sandstones: *Geophys.Prospecting*, **47**, 487-508.

Landrø, M., 2001, Discrimination between pressure and fluid saturation changes from time-lapse seismic data*: Geophysics, Soc. of Expl. Geophys.,* **66**, 836-844.

Loures, L.G.C.L., Moraes, F.S., 2005, Effective porosity inference and lithological classification of siliciclastic sandstones from multiple well-log data. *Submitted for Geophysics.*

MacBeth, C., Ribeiro C., 2005, The stress sensitivity of unsaturated shaley sandstones. *Submitted for Geophys Prospecting.*

MacBeth, C., 2004, A classification for the pressure-sensitivity properties of a sandstone rock frame. Geophysics, **69**, 497–510.

MacBeth, C., Stephen, K.D., and McInally, A., 2005, The 4D signature of OWC movement due to natural production in a stacked turbidite reservoir, *Geophys Prospecting*, **53***,* 183-203

Tura and Lumley 1999, Estimating pressure and saturation changes from timelapse AVO data: *61th Ann. Conf., Eur. Assoc. Geosci. Eng., Extended Abstracts*, paper 1–38.